

The Inactive Typhoon Season of 2010

Hiroataka Kamahori

Meteorological Research Institute, Japan Meteorological Agency

1. Introduction

Tropical cyclones (TCs) are recognized as extreme meteorological phenomena due to the heavy rainfall and strong winds they bring, and are a cause of social concern in countries they influence. The Japan Meteorological Agency (JMA) has monitored TC activity and maintained related records since 1951. According to these statistics, the annual normal for the number of TCs generated in the western North Pacific is 26.7.

Only 14 TCs formed in 2010, representing the lowest total since JMA began its TC monitoring activities in 1951 and beating the previous minimum of 16 recorded in 1998. Nakazawa (2001) discussed the relationship between the number of TC formations and large-scale atmospheric circulation fields in the tropical Pacific to examine why there were so few tropical cyclones in 1998, and identified relatively unfavorable circulation fields for their formation in the tropical western Pacific due to divergence fields influenced by the anomalous Walker circulation. This is a typical example of TC formation being strongly governed by large-scale circulation in the tropical region.

Here, the reasons for the low number of TC formations in 2010 compared to that of 1998 are discussed.

2. Data

This section discusses 2010 TC activity from the viewpoints of atmospheric circulation, sea surface temperature (SST) and precipitation. The Japanese 25-year Reanalysis (JRA-25) and JMA's Climate Assimilation System (JCDAS) (Onogi et al., 2007) are used for atmospheric data, and the Centennial in-situ Observation Based Estimates of variability of global Sea Surface Temperature (COBE-SST) (Ishii et al., 2005) are used for SST values. For JRA-25/JCDAS and COBE-SST, the climatological values are defined as the averages for the period 1979 – 2004. As precipitation data, the Tropical Rainfall Measuring Mission (TRMM)/3B42 set (Huffman et al., 2007) is used. As the available data in this set are from after 1998, its climatology are defined as the averages for the period 1998 – 2010. JMA best track data are used for TC information, and normal TC formation values averaged for the period 1971 – 2000 are adopted.

Table 1 Years with record-low numbers of TC formations. Numbers in parentheses indicate the deviation from the normal (26.7).

| Rank | Year | TC formations |
|------|------|---------------|
| 1 | 2010 | 14 (-12.7) |
| 2 | 1998 | 16 (-10.7) |
| 3 | 1969 | 19 (-7.7) |
| 4 | 2003 | 21 (-5.7) |
| 4 | 1977 | 21 (-5.7) |
| 4 | 1975 | 21 (-5.7) |
| 4 | 1973 | 21 (-5.7) |
| 4 | 1954 | 21 (-5.7) |
| 4 | 1951 | 21 (-5.7) |

3. Annual number of TC formations

Table 1 lists years with record-low numbers of TC formations since 1951, and shows that the total has

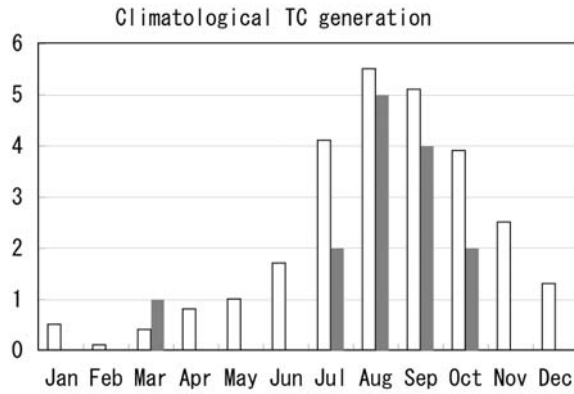


Figure 1 Normal monthly TC formations (white) and those for 2010 (shaded). Normal values are defined as the averages for 1971 – 2000.

Table 2 Seasonal TC formation statistics for the normal, 2010 and 1998. Numbers in parentheses indicate the deviation from the normal.

| Season | Normal | 2010 | 1998 |
|-----------------------|--------|-----------|----------|
| Winter Jan. – Mar. | 1.0 | 1 (+0.0) | 0 (-1.0) |
| Spring Apr. – Jun. | 3.5 | 0 (-3.5) | 0 (-3.5) |
| Summer Jul. – Sep. | 14.6 | 11 (-3.6) | 9 (-5.6) |
| Autumn Oct. – Dec. | 7.7 | 2 (-5.7) | 7 (-0.7) |

been below 20 only three times (in 1969, 1998 and 2010) during the period. As the standard deviation for annual TC formation variability is 4.6, the TC formation anomaly of -12.7 seen in 2010 corresponds to a value of -2.8 after normalization with the standard deviation. If the number of annual TC formations follows Gaussian distribution, the probability of an absolute normalized anomaly larger than 1.83 is less than 1/30, and can therefore be seen as an extreme. The TC formation anomaly of -10.7 seen in 1998 corresponds to a normalized value of -2.3, and can also be regarded as an extreme event. There are two extreme events with an occurrence frequency of 1/30 (1998 and 2010) for the 60-year period from 1951 to 2010, which is consistent with the expected frequency of extreme phenomena. Accordingly, it is reasonable to assume that the annual TC formation variability can be approximated based on Gaussian distribution.

Figure 1 shows the number of monthly TC formations in a normal year and in 2010. Four characteristic TC seasons can be identified: April to June, when the number of formations increases as the season progresses; July to September, which is the peak formation season; October to December, when the number of formations decreases as the season progresses; and January to March, which is the minimum formation season. Accordingly, April to June is defined as spring, July to September as summer, October to December as autumn, and January to March as winter for discussion of seasonal TC formations. Table 2 shows the number of seasonal formations for a normal year, for 2010, and for 1998. In 1998, there were no TC formations in winter and spring, and only a small number in summer. However, the number of formations in

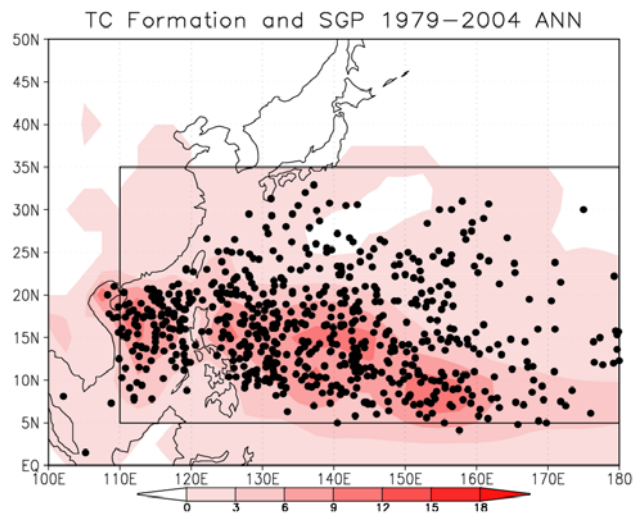


Figure 2 Distribution of annual SGP climatology values (shading) and TC formation positions (dots) for 1979 – 2004. The rectangular area defines the region shown in figures 4, 5, 6, 7 and 13.

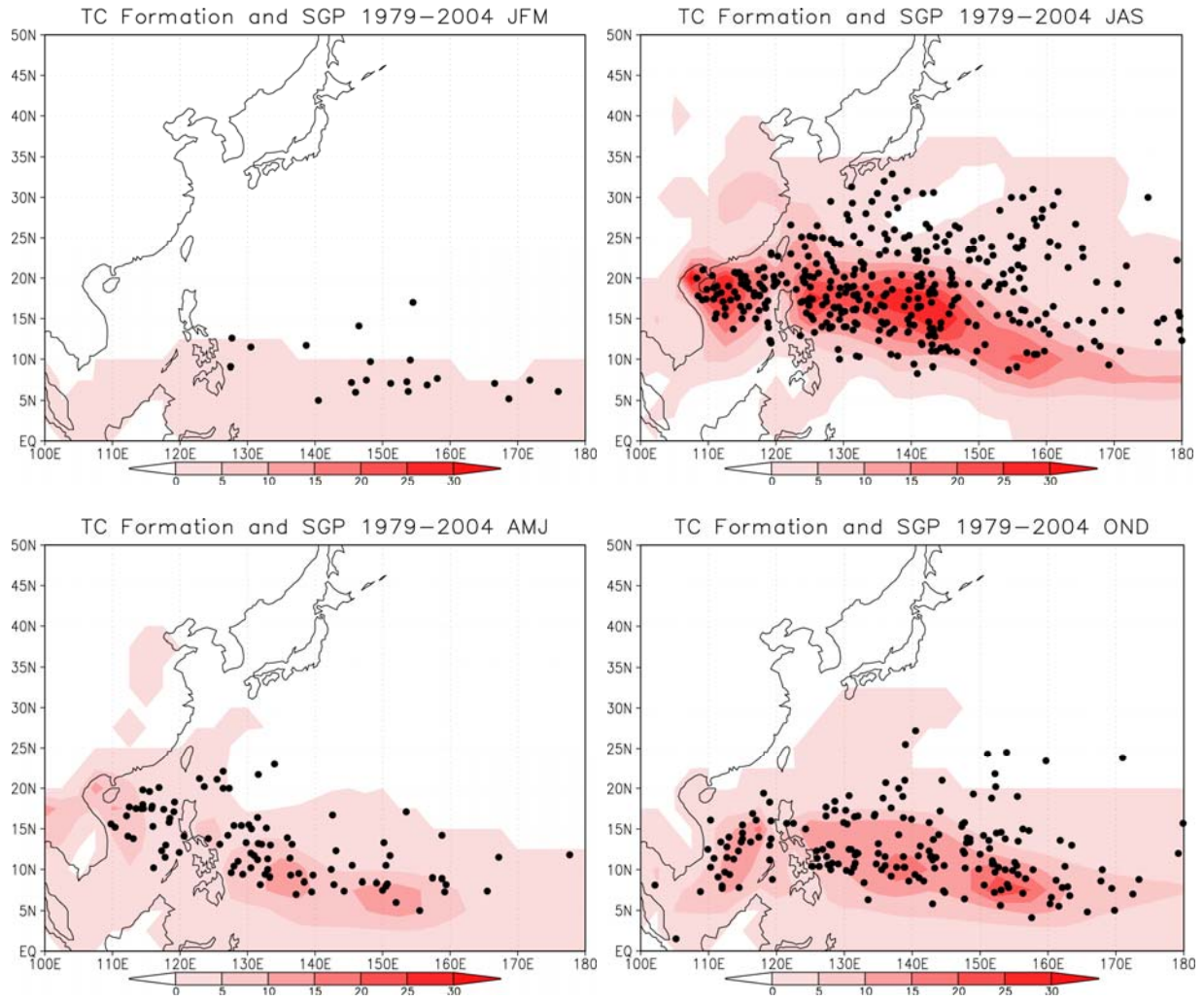


Figure 3 Seasonal distribution of SGP and TC formation positions in winter (Jan. – Mar.; upper left), spring (Apr. – Jun.; lower left), summer (Jul. – Sep.; upper right), and autumn (Oct. – Dec.; lower right)

autumn was comparable with the normal. In 2010, there were few formations throughout the year, and only a third of the normal number in autumn. It is clear that the low number of formations in all seasons of 2010 resulted in the new record-low total.

4. TC genesis potential

It is natural to assume that TC formation frequency is significantly affected by large-scale circulation, and researchers have long tried to quantify the influence of this. As a parameter for defining TC formation frequency, Gray (1979) introduced the non-dimensional seasonal genesis parameter (SGP), consisting of three kinematic and three thermodynamic parameters:

- (1) Relative vorticity in the lower troposphere (P_{vr})
- (2) Coriolis parameter (P_f)
- (3) Vertical wind shear over the whole troposphere (P_{vs})
- (4) Ocean energy (P_{oc})

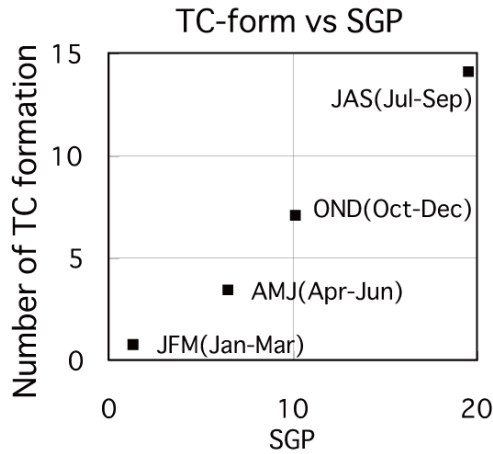


Figure 4 Relationship between the climatology of seasonal TC formation frequency and the seasonal SGP averaged over 5°N – 35°N and 110°E – 180°E

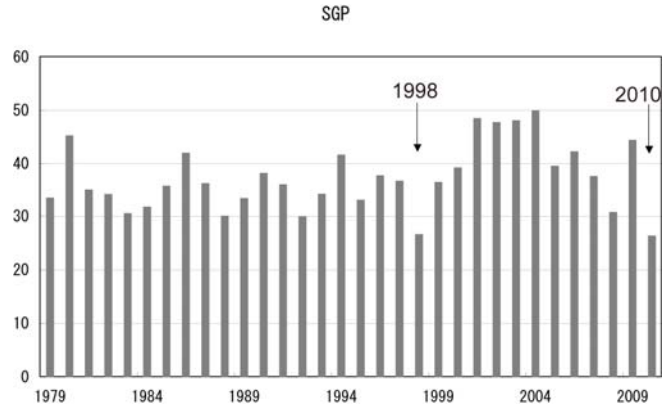


Figure 5 Year-to-year variation of annual SGP averaged over 5°N – 35°N and 110°E – 180°E

- (5) Moist stability in the middle troposphere (Pms)
- (6) Relative humidity in the middle troposphere (Prh)

Figure 2 shows the annual values of the climatological SGP and TC formation positions for the period 1979 – 2004. Here, the annual SGP is defined as the annual average of the monthly values. The TC formation position is defined as the first position in which the maximum wind speed exceeded 34 kt in the best track of JMA. In Figure 2, the TC formation area shows a close correlation with the large-value region of the SGP over the Philippine Sea and the South China Sea. Accordingly, it can be concluded that the SGP describes the climatological TC formation area well.

Figure 3 shows the seasonal distribution of the SGP and TC formation positions. In winter (Jan. – Mar.) and spring (Apr. – Jun.), the formation frequency is relatively low, as is the SGP value. The relatively large SGP area is distributed in a latitude band on the equator side of 15°N, and corresponds closely to the TC formation area. In summer (Jul. – Sep), the latitude band of the maximum SGP moves northward, and its values become large. The TC formation area also moves northward, and the formation frequency becomes significantly larger than before. Accordingly, it can be assumed that the SGP closely represents the seasonal TC formation frequency and its latitude band in qualitative terms.

Figure 4 shows a scatter diagram for the climatology of the seasonal mean SGP averaged over 5°N – 35°N and 110°E – 180°E (the rectangular area shown in Figure 2) and the climatology of the seasonal TC formation frequency. As the values show close proportionality, it can be concluded that the SGP reasonably describes the seasonal progress of TC formation frequency. As it can be concluded that the SGP closely represents the distribution of the TC formation area and the number of seasonal TC formations in the climatology, the next question would be whether the SGP explains year-to-year variations in the number of TC formations.

Figure 5 shows year-to-year variations in the annual SGP. In 1998 and 2010, when the number of TC formations was significantly lower than the climatology, the SGP values were also significantly small. The

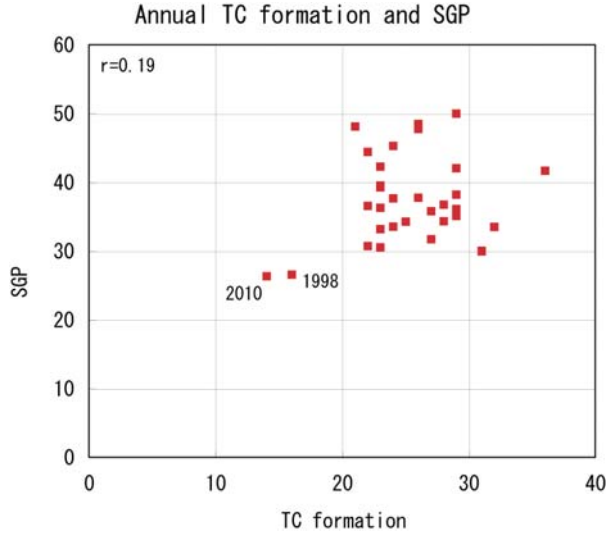


Figure 6 Scatter diagram showing the annual mean SGP averaged over 5°N – 35°N and 110°E – 180°E and the annual TC formation frequency.

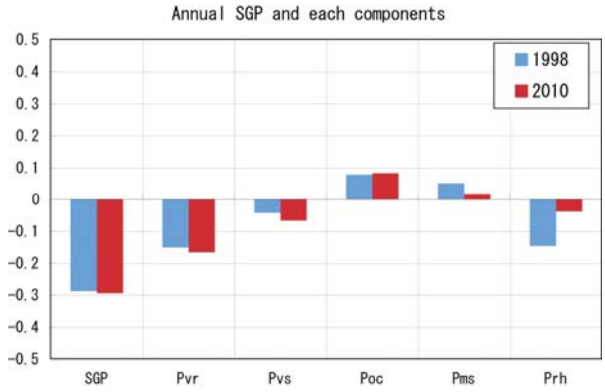


Figure 7 Annual anomalies of the SGP and its components in 2010 and 1998 averaged over 5°N – 35°N and 110°E – 180°E.

climatology for the annual SGP is around 37, and its standard deviation is 6.3. The SGP anomaly for 2010 is -10, which corresponds to a normalized value of -1.8 with the standard deviation, and this is comparable with the normalized number of TC formation anomaly (-2.6). Figure 6 shows a scatter diagram with the annual SGP and the annual number of TC formations. The coefficient of correlation between the two values is 0.19, which is not statistically significant. Although the SGP explains the climatological characteristics of TC formation well, it does not explain year-to-year variations in TC activity. The standard deviation for the number of annual TC formations is 4.6, which is only 1/6 of the number of annual formations. Other factors not included in the SGP may contribute to this low variation. However, it is true that the SGP is very small when the number of TC formations is also very small, as seen in 2010 and 1998. This fact and the reproducibility of the climatological seasonal TC formation shown in Figure 3 support the idea that extreme variability in TC formation compared with the climatology is described by the SGP. Based on this background, the following sections discuss the reason for the extremely low number of TC formations seen in 2010 based on the SGP and its components.

5. Number of TC formations and the SGP in 2010

Figure 7 shows annual anomalies in the SGP and its components for 2010 and 1998. No panel is shown for the Coriolis parameter because it is constant. It can be seen that the SGPs in 2010 and 1998 were 30% smaller than the climatology. As a feature common to both years, the largest contribution to negative SGP anomalies is from the vorticity parameter. Figure 8 shows a scatter diagram with annual numbers of TC formations and annual vorticity parameters. The coefficient of correlation between the annual vorticity parameters and the numbers of TC formations is 0.56, which is significant at the 95% level. In 2010 and 1998, the vorticity parameters were considerably smaller than those in other years, and it is assumed that this parameter contributed significantly to the negative anomalies in the numbers of TC formations for both years. Figure 9 shows the climatological distribution of relative vorticity for 850 hPa and TC formation positions for summer (Jul. – Sep.) over the western Pacific and the Indian Ocean. The TC formation

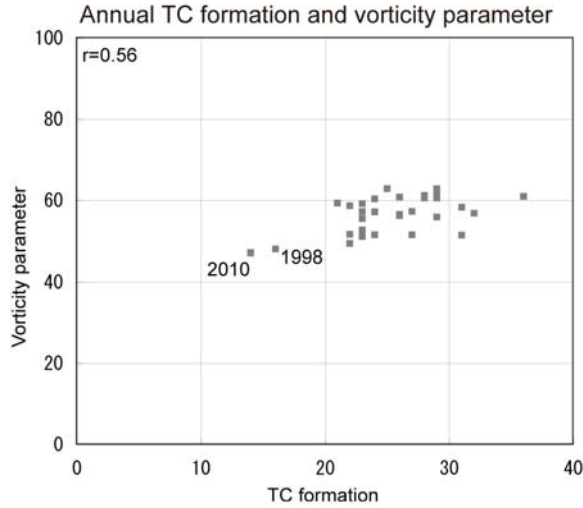


Figure 8 Scatter diagram showing the number of TC formations and annual vorticity parameters averaged over 5°N – 35°N and 110°E – 180°E

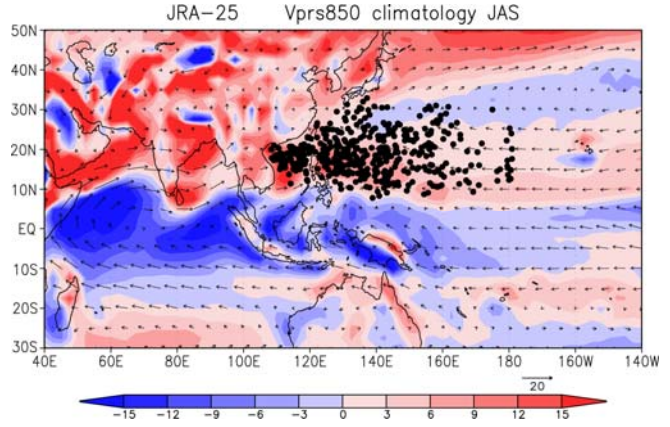


Figure 9 Climatological relative vorticity at 850 hPa in units of 10^{-6} s^{-1} (shading) and horizontal wind (arrows) at 850 hPa in summer (Jul. – Sep.). The dots indicate TC formation locations in summer for the period 1979 – 2004.

positions are mainly distributed over the South China Sea and the tropical Pacific east of the Philippines, where cyclonic vorticity is dominant. Accordingly, the importance of vorticity on the number of TC formations in the climatology is assumed.

Conversely, the oceanic energy parameter shows positive anomalies both in 2010 and 1998, and indicates positive anomalies in the number of TC formations – a tendency opposite to that of the SGP. Figure 10 shows SST anomalies in the western Pacific and the Indian Ocean for the summers (Jul. – Sep.) of 2010 and 1998. A La Niña event occurred in 2010, and anomalous negative SSTs were distributed over the eastern and central equatorial Pacific, with positive anomalies in the western equatorial Pacific. Accordingly, positive SST anomalies were seen in the Philippine Sea and the South China Sea as climatological TC formation areas. In 1998, the El Niño event retreated in the first half of the year, and the onset of a La Niña event was seen in the second half. In the summer of 1998, there were lower SSTs in the eastern and central equatorial Pacific and higher values in the South China Sea and the Philippine Sea, as in summer 2010. In 2010 and 1998, the numbers of TC formations were significantly lower than the climatology despite the higher SSTs in the TC formation area. Although the influence of SSTs on TC formation is clear, it should be understood that other parameters also play an important role, and that TC formation is restricted by these parameters despite relatively high SSTs. Another important consideration is the positive SST anomaly distribution seen around the Maritime Continent and the eastern Indian Ocean. This point will be discussed later.

Based on these discussions, it is clear that vorticity plays an important role in TC formation in addition to SSTs. The next section discusses why vorticity fields were so much less significant than their climatology in the western North Pacific for 2010.

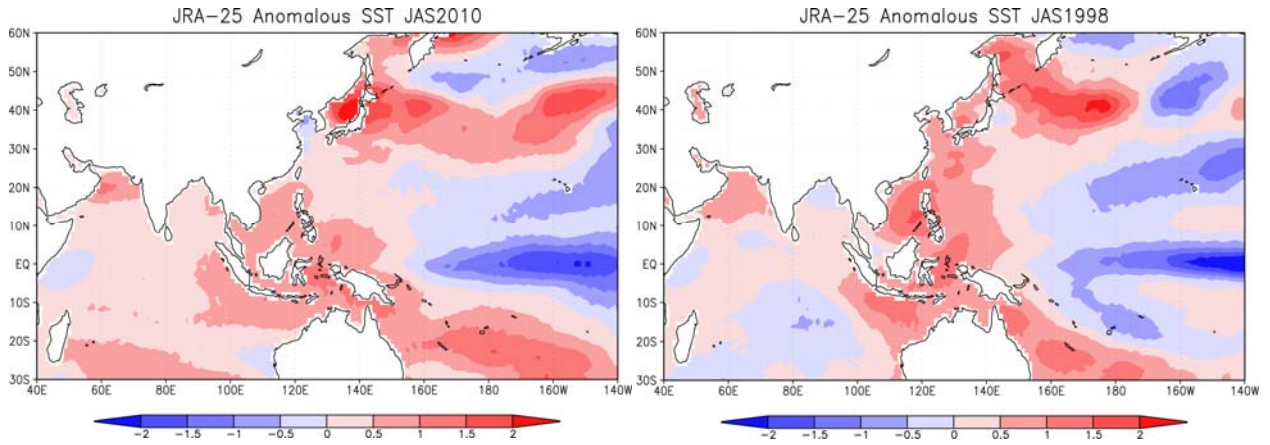


Figure 10 SST anomalies in summer 2010 (left) and summer 1998 (right)

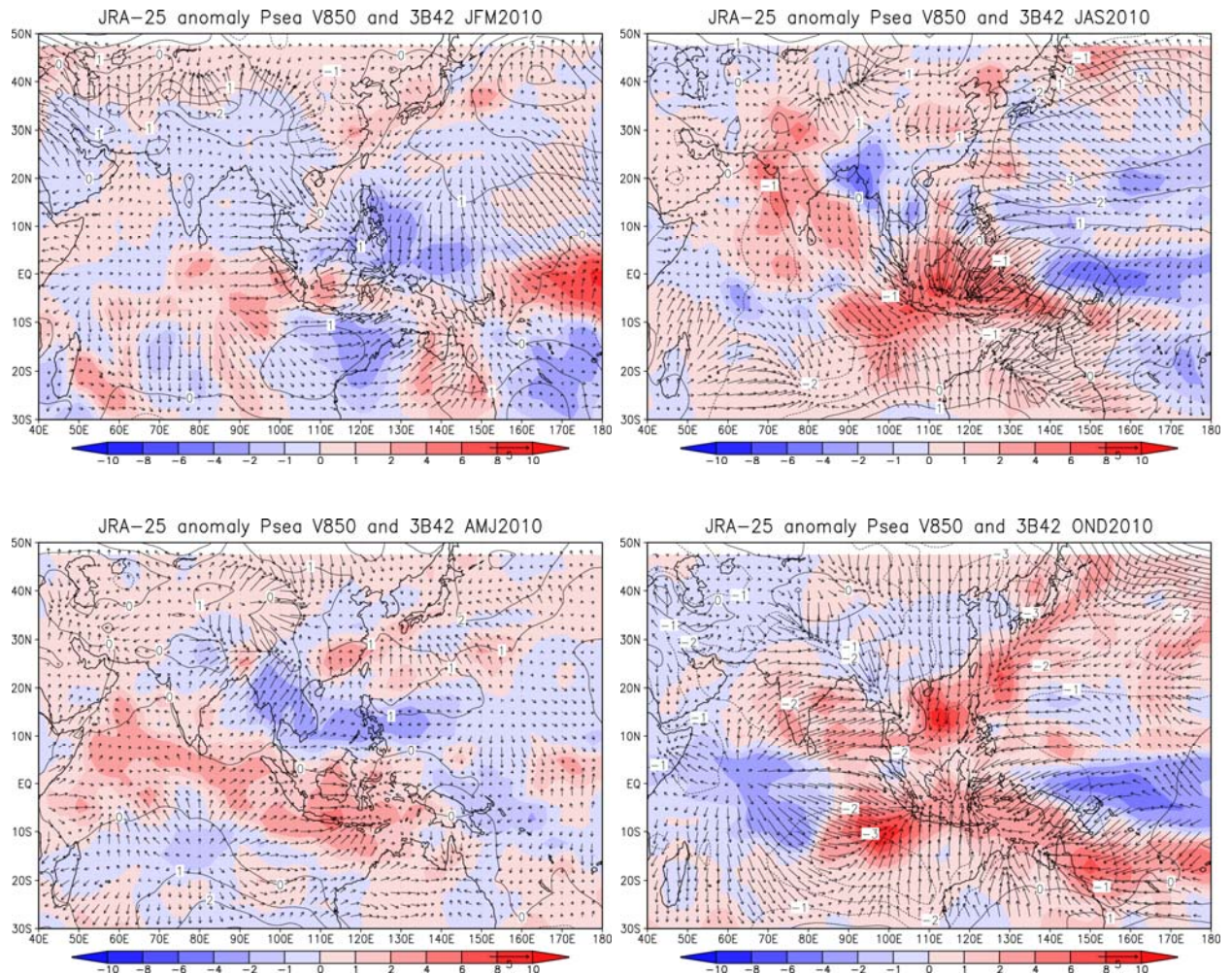


Figure 11 Mean sea level pressure anomalies in units of hPa (contour lines), divergent wind anomalies at 850 hPa, and precipitation anomalies in units of mm day^{-1} (shading) in winter (Jan. – Mar.; upper left), spring (Apr. – Jun.; lower left), summer (Jul. – Sep.; upper right) and autumn (Oct. – Dec.; lower right) of 2010

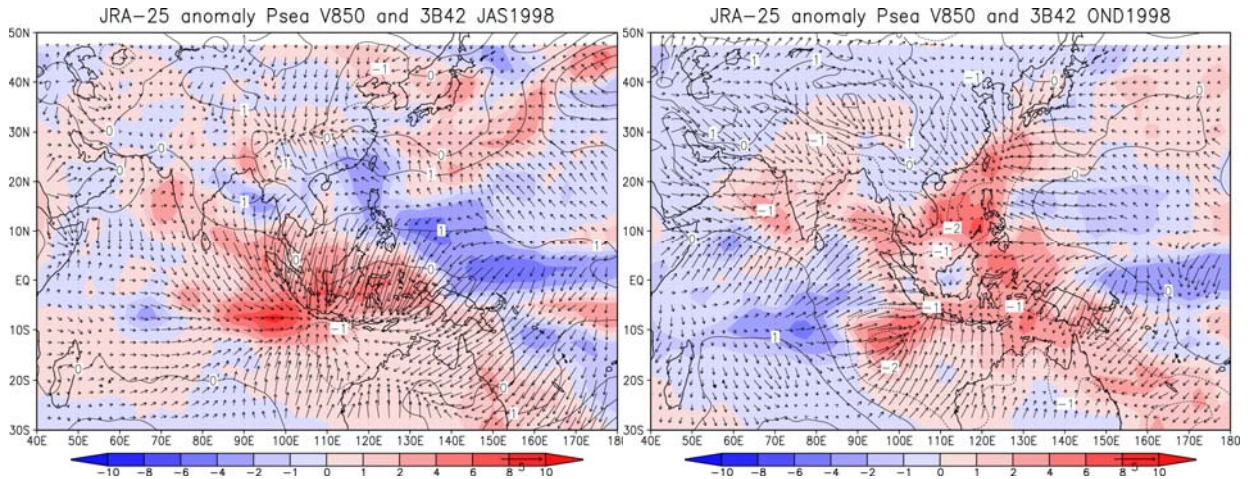


Figure 12 As per Figure 11, but for summer (Jul. – Sep.; left) and autumn (Oct. – Dec.; right) of 1998 only.

6. Large-scale atmospheric circulation in relation to TC formation

Figure 11 shows seasonal sea level pressure anomalies, divergent wind anomalies at the 850-hPa level, and precipitation anomalies over the western Pacific and the Indian Ocean in 2010. In winter, spring and summer, anti-cyclonic circulation anomalies were seen over the Pacific south of Japan, and negative precipitation anomalies occurred in these regions. In response, the lower troposphere in most of the western North Pacific exhibited relatively divergent circulation fields. Conversely, there were convectively active areas over the Maritime Continent and the eastern Indian Ocean, which is on the southwest side of the divergent circulation areas. This meant that convective activity was suppressed and the lower troposphere exhibited divergent circulation in the western North Pacific, and these diverged atmospheric conditions tended to converge around the Maritime Continent and the eastern Indian Ocean. Especially in the summer (Jul. – Sep.), when TC formation is the most active, anti-cyclonic surface pressure anomalies extended significantly to the western North Pacific, and cyclonic surface pressure anomalies were distributed over the Maritime Continent and the eastern Indian Ocean. As a result, large-scale anomalous flow from the Northern Hemisphere to the equatorial region and the Southern Hemisphere occurred in the lower troposphere. In autumn, the Pacific subtropical anti-cyclone weakened rapidly, and negative surface pressure anomalies extended to the whole of the western North Pacific. As a result, convective activity increased in the South China Sea. However, negative anomalies of sea level pressure persisted over the Maritime Continent and the eastern Indian Ocean, and the large-scale flow from the Northern Hemisphere to the Southern Hemisphere continued in the lower troposphere. As a result, divergent circulation continued over the Philippine Sea (the main TC formation area in the region), thereby suppressing TC activity.

Throughout 2010, lower tropospheric flow toward the Southern Hemisphere from the Northern Hemisphere was seen, and the climatological TC formation area was governed by divergent circulation. As a result, the vorticity parameter in the western North Pacific was quite small, which led to suppressed TC activity throughout the year.

For comparison, the divergence field for 1998 was also investigated. Figure 12 shows anomalies of sea level pressure, divergent wind at 850 hPa, and precipitation over the western Pacific and the Indian Ocean

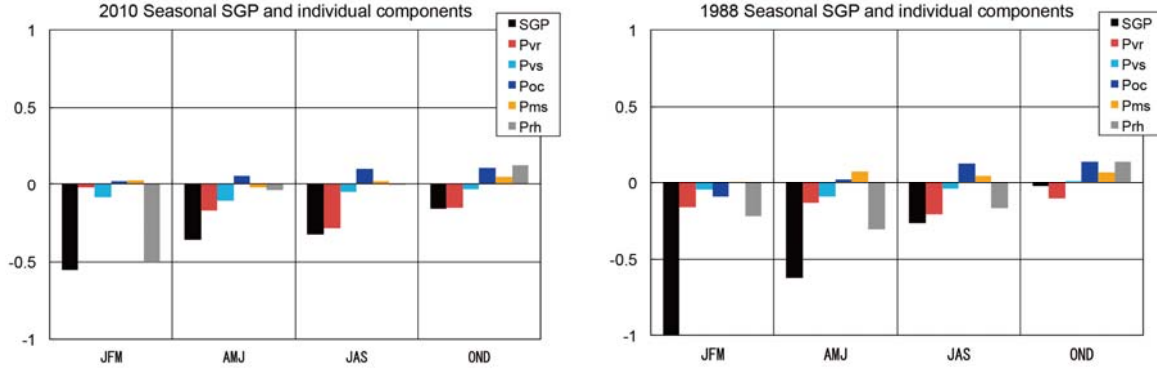


Figure 13 Normalized seasonal area mean SGP and its components for 1998 (right) and 2010 (left). The averaged area is specified in Figure 2. JFM, AMJ, JAS and OND indicate winter (Jan. – Mar.), spring (Apr. – Jun.), summer (Jul. – Sep.), and autumn (Oct. – Dec.), respectively.

in the summer and autumn of 1998. During the summer, anti-cyclonic circulation anomalies were seen over the Pacific south of Japan, and cyclonic anomalies were observed over the eastern Indian Ocean. Positive precipitation anomalies were seen over the Maritime Continent and the eastern Indian Ocean, and a large-scale flow from the western North Pacific to the Maritime Continent and the Indian Ocean formed, creating anomalous fields similar to those of summer 2010.

In the autumn of 1998, the Pacific subtropical anti-cyclone weakened and the lower tropospheric flow from the western North Pacific to the eastern Indian Ocean retreated. As a result, cyclonic circulation and positive precipitation anomalies were seen over the South China Sea and the Philippine Sea.

As shown in Table 2, only nine TCs formed in the summer of 1998, representing just 60% of the climatology. However, seven formations were seen in autumn, which is comparable with the climatology. This is in contrast to the situation seen in 2010, when the number of autumn formations was low. This observation was discussed from the viewpoint of the SGP. Figure 13 shows the normalized seasonal mean SGP and its components for 1998 and 2010. Here, the averaged domain is $5^{\circ}\text{N} - 35^{\circ}\text{N}$ and $110^{\circ}\text{E} - 180^{\circ}\text{E}$, as shown in Figure 7. For 2010, the SGP shows very large negative anomalies throughout the year. In summer and autumn in particular, negative anomalies in the vorticity parameter contributed significantly to the negative values in the SGP. In the summer of 1998, the vorticity parameter contributed to negative anomalies in the SGP as seen in the summer of 2010, but the absolute value of the negative vorticity parameter approached the climatology in autumn. As a result, the SGP also tended toward the climatology in autumn. That is, due to weakening of the large-scale lower tropospheric flow from the western North Pacific to the Indian Ocean, low convective activity in the western North Pacific retreated, and the vorticity parameter tended toward the climatology, which resulted in normal TC formation in the autumn of 1998. In contrast, the large-scale flow from the western North Pacific to the Indian Ocean persisted, resulting in a large negative vorticity parameter and suppressed TC activity in the autumn of 2010.

The relationship between conditions in the western North Pacific and the Indian Ocean in 2010 and 1998 is verified from the viewpoint of large-scale circulation. Figure 14 shows climatological 200-hPa velocity potential fields and the TC formation locations in summer and autumn (upper), along with 200-hPa velocity potential anomalies and the TC formation locations in the summer/autumn seasons of 2010 and 1998

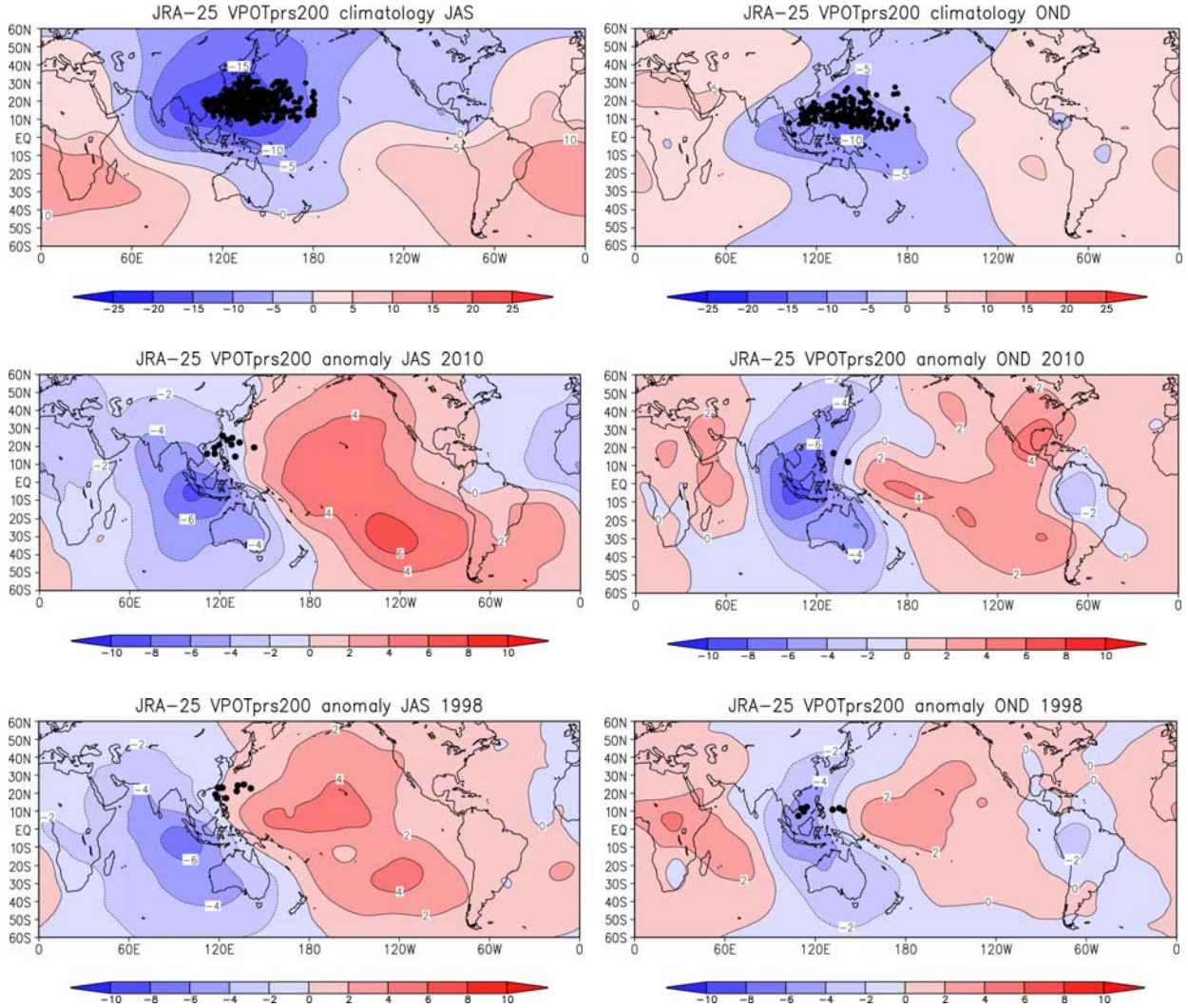


Figure 14 Upper left and right: 200-hPa velocity potential field climatology and TC formation locations for the period 1979 – 2004 in summer and autumn. Middle left and right: 200-hPa velocity potential anomalies and TC formation locations for summer and autumn 2010. Lower left and right: 200-hPa velocity potential anomalies and TC formation locations for summer and autumn 1998.

(middle and lower). In the climatology, the tropical upper tropospheric divergence area corresponds closely to the TC formation locations both in summer and in autumn. As the upper tropospheric divergence fields correspond to the lower tropospheric convective activity, it is assumed that TC formation occurs in the large-scale area of convective activity. It is also notable that this area is located at a more northerly latitude in summer than in autumn, as are the TC formations locations.

In the summer of 2010, upper tropospheric convergent anomalies were seen over the whole of the Pacific, while divergent anomalies were observed over the whole of the Indian Ocean. As a result, the area of convective activity was displaced from the western North Pacific to the Indian Ocean. It is assumed that the low convective activity over the western North Pacific resulted in the low number of TC formations in the summer of 2010. In the summer of 1998, upper tropospheric divergence anomalies similar to those

observed in the summer of 2010 were recorded, and TC activity was suppressed by similar factors. In 2010, upper tropospheric convergent anomalies over the Pacific persisted in autumn, and TC activity was also suppressed. In Figure 14, negative velocity potential anomalies are seen around the South China Sea and the Philippines. However, velocity potential is an integrated quantity, so the important point is its horizontal gradient rather than its positive or negative status.

In the autumn of 1998, the contrast in the upper tropospheric divergence fields between the Pacific and the Indian Ocean weakened. As a result, the displacement of the convectively active area to the Indian Ocean retreated, convective activity increased in the western North Pacific, and the number of TC formations reverted toward the climatology.

7. Summary and discussion

This study examined why the number of TC formations in 2010 was the lowest on record since JMA began monitoring TC activity in 1951. The annual value of the SGP over the western North Pacific in 2010 was the lowest on record since 1979. The second-lowest value was recorded in 1998, which also saw the second-lowest number of TC formations. In both years, lower tropospheric vorticity was significantly below the climatology, which resulted in lower SGP values and fewer TC formations. Even though the SST in the TC formation area was higher than the climatology, convective activity was more suppressed and vorticity was below the climatology in both years. This suppressed convective activity is considered to have stemmed from a large-scale flow from the Northern Hemisphere to the Southern Hemisphere and divergent circulation in the western North Pacific along with convergent circulation in the eastern Indian Ocean persisted throughout the year. As a result, the convectively active area in 2010 was shifted from the South China Sea and the Philippine Sea toward the Maritime Continent and the eastern Indian Ocean. Also in the summer of 1998, a similar pattern of circulation deviation formed between the western North Pacific and the eastern Indian Ocean, but weakened in autumn. Conversely, circulation deviation persisted throughout the whole of 2010, resulting in a record-low number of TC formations. Although TC activity is known to show a close proportional relationship to SST, it is important to consider that it is also affected by large-scale tropical circulation. As a result, the number of TC formations may in fact be lower despite higher SSTs.

References

- Gray, W. M., 1979: Hurricanes: Their formation, structure, and likely role in the tropical circulation. *Meteorology over the Tropical Oceans*, D. B. Shaw, Ed., Royal Meteorological Society, 155 – 218.
- Huffman, G. J., R. F. Adler, D. T. Bolvin, G. Gu, E. J. Nelkin, K. P. Bowman, Y. Hong, E. F. Stocker, D. B. Wolff, 2007: The TRMM Multisatellite Precipitation Analysis: Quasi-Global, Multiyear, Combined-Sensor Precipitation Estimates at Fine Scale. *J. Hydrometeor.*, 8, 38 – 55. doi: 10.1175/JHM560.1
- Ishii, M., A. Shouji, S. Sugimoto and T. Matsumoto, 2005: Objective analyses of sea-surface temperature

- and marine meteorological variables for the 20th century using ICOADS and the Kobe Collection. *Int. J. Climatol.*, 25, 865 – 879. doi: 10.1002/joc.1169.
- Nakazawa, T., 2001: Suppressed Tropical Cyclone Formation over the Western North Pacific in 1998. *J. Meteor. Soc. Japan*, 79, 173 – 183. doi: 10.2151/jmsj.79.173.
- Onogi, K., J. Tsutsui, H. Koide, M. Sakamoto, S. Kobayashi, H. Hatsushika, T. Matsumoto, N. Yamazaki, H. Kamahori, K. Takahashi, S. Kadokura, K. Wada, K. Kato, R. Oyama, T. Ose, N. Mannoji and R. Taira, 2007: The JRA-25 Reanalysis. *J. Meteor. Soc. Japan*, 85, 369 – 432. doi: 10.2151/jmsj.85.369.